A 3-Axis Optical Force/Torque Sensor for Prostate Needle Placement in Magnetic Resonance Imaging Environments

Hao Su, Gregory S. Fischer

Abstract— **The work presented in this paper has been performed in furtherance of developing an MRI (Magnetic resonance imaging) compatible fiber optical force sensor. In this paper, we discuss the design criteria and sensing principle of this optical sensor for monitoring forces in the 0-20 Newton range with an sub-Newton resolution. This instrumentation enables two degrees-of-freedom (DOF) torque measurement and one DOF force measurement. A novel flexure mechanism is designed and the finite element analysis is performed to aid the optimization of the design parameters. This 3 axis force/torque sensor with this range and resolution is an ideal tool for interventional procedures, e.g. needle biopsy and brachytherapy. The sensor is experimentally investigated and calibrated. Calibration results demonstrate that this sensor is a practical and accurate measurement apparatus.**

I. Introduction

The MRI based medical diagnosis and treatment paradigm capitalizes on the novel benefits and capabilities created by the combination of high sensitivity for detecting tumors, high spatial resolution and high-fidelity soft tissue contrast. This makes it an ideal modality for guiding and monitoring medical procedures, such as needle biopsy and low-dose-rate permanent brachytherapy. Though with so many appealing merits, the magnetic and electrical fields in MRI environment presents significant challenges for mechatronic instrumentation design. Generally, the development of sensors for applications in MR environments requires careful consideration of safety and electromagnetic compatibility constraints. Fig.1 illustrates a diagram of a traditional transrectal ultrasound guided (TRUS) brachytherapy needle placement procedure which is structurally similar to our application in [1]. Our previous work in [2] has developed an MRI-compatible actuation system, specifically targeting the neural intervention procedure, we intend to extend this work to sensor design to further our systematic approach to developing MR-compatible mechatronic systems. Specifically, for soft tissue needle placement, our basic measurement requirement is 3 axis hybrid sensing- one force and two torque measurements and the details would be explained in Section II.

Many variants of force sensors are possible, based on different sensing principles and the application scenarios. Table I summarizes recent force sensor and their characteristics. Liu et. al. [4] developed a hydrostatic water pressure transducer to infer grip force. Takahashi et. al. [5] have developed an six axis optical force/torque sensor based on differential light intensity, and the sensor was used for brain function analysis. A large number of fibers are necessary in this design and its nonlinearity and hysteresis are conspicuously undesirable. A newer generation optical force sensor by Tada and Kanade [6] has prominent advantages over the previous design in which the light source and the sensing device are placed on separate bases and their relative displacement is measured. The number of fibers was reduced to two for 2-DOF displacement measurements with magnified flexure deformation. The most recent development from the same group was reported in [7] and it demonstrated a uni-axial sensor with redesigned flexible structure taking account of the axial interference. These two designs are 3-axial and uni-axial force measurement respectively.

A 2-DOF force measurement mechanism based on reflected light intensity is presented in [8]. The measurement of the deflection of an elastic body is performed by sending light from an emitting fiber to a moving mirror. A novel optical fiber Bragg grating (FBG) sensor somewhere was developed by Park et. al. [9]. It is credited for MRI-compatible, but it has higher accuracy than what we need in the cost of very expensive support electronics. Puangmali and co-workers [10] presented a 3-axis force sensor based

Hao Su and Gregory S. Fischer are with the Automation and Interventional Medicine (AIM) Laboratory in the Department of Mechanical Engineering, Worcester Polytechnic Institute, Worcester, MA, USA gfischer@wpi.edu

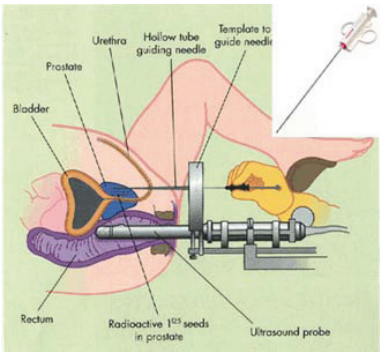

Fig. 1. Brachytherapy diagram with ultrasound guided needle [3] and a typical surgical needle.

TABLE I
Characteristics of existing MRI compatible force sensors

Location	DoF	Sensing Quantity	Sensing mechanism
Cleveland, USA [4]	1	force	hydrostatic pressure
Nara, Japan [5]	6	force/torque	differential light intensity
AIST, Japan[6]	3	force	differential optical fiber
AIST, Japan [7]	1	force	optical micrometry
EPFL, Swiss [8]	2	force	absolute light intensity
Stanford, USA [9]	1	force	optical fiber Bragg grating
London, UK [10]	3	force	optics

978-1-4244-4992-7/09/$25.00 ©2009 IEEE

on an optical sensing principle. The sensor prototype demonstrated uniform force measurement in both axial and radial directions in the ranges of ± 3 N, while in needle placement application, a much larger range is required. For further details, we refer the readers to [11] for a comprehensive review of sensors in magnetic resonance environment.

None of the aforementioned force sensors (except the high-cost fiber Bragg sensor) in MR environment satisfy the stringent requirement for needle placement, and as to the authors' knowledge, our design is the first prototype with hybrid (one axis force and two axis torque) sensing capability for interventional needle-based procedures.

One salient challenge in this design is the compromise of measuring capability and accuracy. Our application needs the measurement of two lateral torques and one axial force, while from Table I, we observe that this is not trivial with guaranteed accuracy. One approach is to follow the idea of [5] to design a generic 6 DOF force sensor which is potentially not compact enough to provide suitable tool interface, while another more appealing alternative is to design sub-six DOF force sensor which would specifically satisfy these kind of sensing requirement. We summarize the other imperative design considerations in three aspects. First, ferromagnetic components are attracted by the high spatial magnetic field gradient, so limited materials are eligible for MRI application. Moreover, since the place of interest for patients with prostate pathology are usually placed in the iso-center of scanner, this presents much more stringent design safety and compatibility consideration then most of the previously developed MR haptic devices. Third, limited space requires that the sensor should be miniaturized to facilitate integrated usage. The article is organized as follows. Section II describes the design criteria and sensing principle and Section III describes the detailed design of system prototype. Calibration results are presented in Section IV, with a discussion of the sensor in Section V.

II. Sensing Principle

A. Design Criteria

Our guiding vision is to create an MRI compatible force sensor for needle-based interventional procedures by a fiber optical module, sensed by a flexible body, while possessing the ability to sense insertion force and detect non-tissue or healthy tissue contact interface to enhance the overall clinical performance. Before designing the force sensor, it is imperative to investigate the sensing DOF, force range and force resolution.

In-vivo needle insertion force measurement is an important precursor to monitor the insertion status, consequently provides significant indicator for force sensor design. Following similar analysis of [12] by Abolhassani et. al., the needle (symmetric or asymmetric) would bend with a very small sloped deflection curve during the insertion, generically, there are 6-DOF forces/torques applied to the needle as shown in Fig.2(a) . The distributed forces orthogonal with respect to each infinitesimal segment of the needle shaft can be considered as a lumped force at the tip. The most important quantities to be sensed are the force along the needle axis and the two resultant torques of the forces tangential to the needle axes.

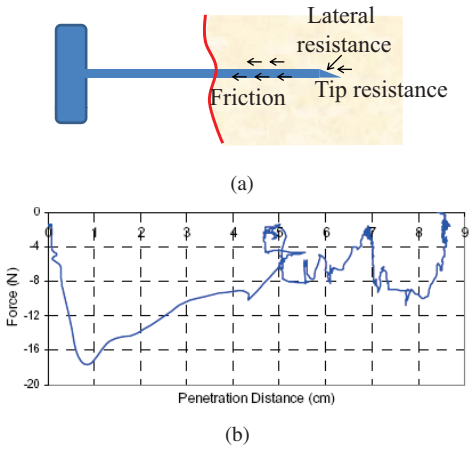

Fig. 2. (a) Forces acting on the insertion needle, (b) A typical *in-vivo* prostate needle insertion force profile. [13]

As for the force range and resolution, it is reported in [13] that continuous rotation could improve the targeting accuracy and reduce insertion force. The force profile in the prostate brachytherapy procedure is illustrated in Fig.2(b). According to this plot and some related literatures, we conclude that the force sensing range is within 20 Newton. A resolution of 0.1 Newton is sufficient in our application.

B. Basic Idea: Optical Micrometry

The optical sensing mechanism deployed here is a economic and succinct structure which uses one spherical mirror and multiple optical fibers. In Fig.3(a) , f is the focal length and c is the center of the spherical mirror. The incident light emitted from a point source would get reflected by the front spherical mirror, while the reflected light can be sensed by the tip of multiple optical fibers which forme in circular pattern.

If we deliberately assign the point source in the focal position, the reflected light would parallel to the optical axis therefore engender maximal light received by the fibers. As shown in Fig.3(b), if the relative axial distance between the light source and mirror decreases, there would be proportional light intensity increase in all of optical fibers which can be monitored by on board electronics. On the other hand, if the mirror rotates along the tangential axes, there will be an asymmetric light intensity variance in the fibers, which can be detected by circuits.

III. Device Design

A. Flexure Design

The flexure converts the applied force and torque into displacement of the mirror thus generating a light intensity change. The structure should be simple to facilitate machining process. There are some possible structures of the sensor in literature. Since we desire measurement symmetry, we use a cylinder structure with engraved elastic curves.

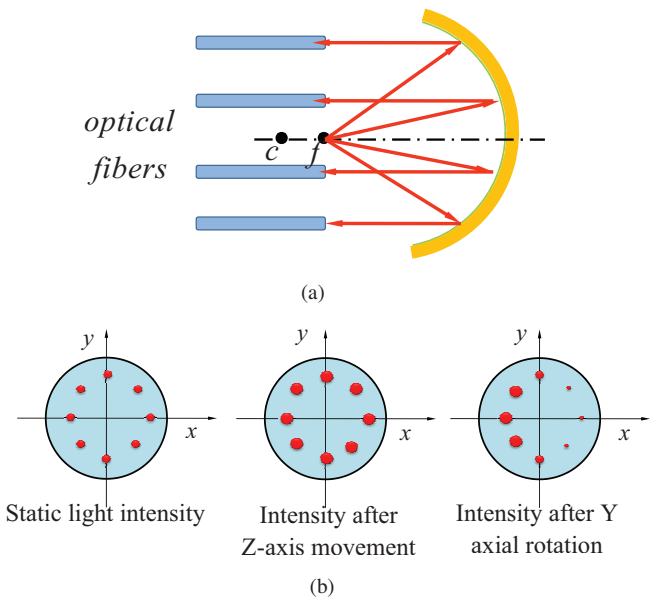

Fig. 3. Sensing mechanism: (a) Light reflection by spherical mirror, (b) Intensity change wit different mirror translation/rotation

Fig. 4. Design of the sensor: (a) The exploded view of the force sensor CAD model,(b) Sensor prototype made of aluminum.

Fig.4(a)shows the exploded view of the force sensor. The sensor has four major components: the fiber holder with eight $1mm$ diameter through holes to arrange the receiver fibers and an additional central hole for the emitter, the flexure, the spherical mirror and an adjustable mirror driver. We want the flexure to sense the axial force and lateral torques with high accuracy while tolerating off-axis forces and torques. It has two parallelogram-like segments of helical circular engravings and this structure has intrinsic axial/ lateral overload protection capability.

B. Adjustable Structure

The reflection of the flat mirror configuration reported in [11] showed the response of these optical sensors as a function of the distance to the mirror has two segments: a linear, high-sensitivity segment in the range below $0.6mm$, and a low, decreasing sensitivity for the higher range above $1mm$. Since a linear response is desired, the sensing part is kept to be within the first segment of the response curve. Though the response curve for spherical mirror is not clear yet, we presumably consider there should be similar issue in this design.

To guarantee high sensitivity and linearity of the sensor, the flexure deflection should be kept within the linear response segment in both directions. On the other hand, it is also desirable to have small deflexion to obtain high stiffness and bandwidth. To this end, we used a plastic screw to fix the mirror holder, thus a simple and accurate adjustment structure by simply screwing the mirror into/out of body of the sensor is accomplished as shown in the right side of Fig. 4(a).

C. Finite Element Analysis

To get a better idea of the design parameters, a number of finite element simulations are performed. The first requirement of this system is that it is MRI-compatible, which means that it is both MRI safe and it will not produce noise and interference with the MRI scanner.

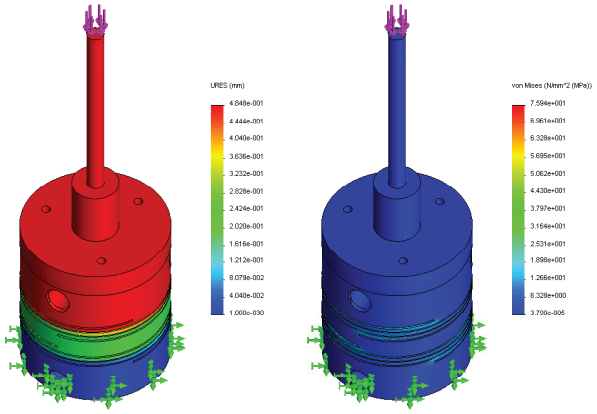

Fig. 5. FEM result with axial 20 Newton force. The left is for the displacement (unit in mm) and the right is for Von Mises stress(unit in N/m^2).

We made a cover plate with a $20mm$ long shaft to mimic the needle structure. In the first simulation, an 20 Newton axial force is applied at the tip of the shaft. The left in Fig.5 shows the sensor displacement while the right one shows

the Von Mises stress. In the second simulation, an 5 Newton lateral force is applied at the tip of the shaft. Fig.6 shows the corresponding sensor displacement and the Von Mises stress correspondingly.

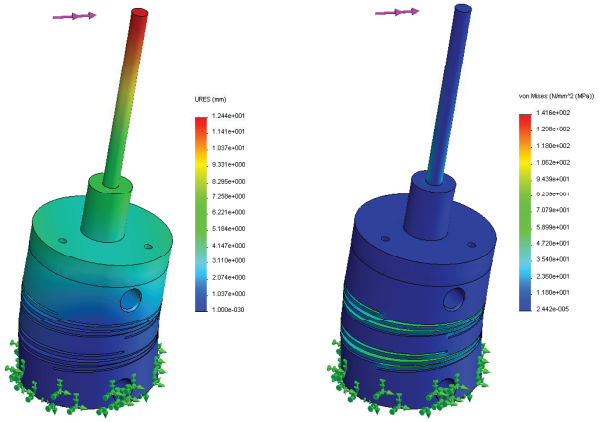

Fig. 6. FEM result with 5 Newton lateral force.The left is for the displacement (unit in mm) and the right is for Von Mises stress (unit in N/m^2).

All the results shows that the sensor displacement is within linear range (here we use the flat mirror response curve), and the martials are capable of this structure and force range.

D. System Implementation

The light signal emitted from a high-output plastic infrared LED (IF-E91A, Industrial Fiber Optics Inc., USA) is reflected by a $9mm$ spherical mirror (Edmund optics ,USA). The emitting position of the LED is designed to be within some desired range of the focus point of the mirror, so the reflected light travels back to the emitting side with maximal intensity, where eight plastic fiber optic photodiodes (IF-D91, Industrial Fiber Optics Inc., USA) are in circular patten to detect the reflected light. The light is transmitted through the plastic optical fiber(SK-40 Super ESKA, Industrial Fiber Optics Inc., USA) with $1mm$ cladding diameter to the electronic board outside of the scanner room. The sensor prototype is shown in Fig.4(b).

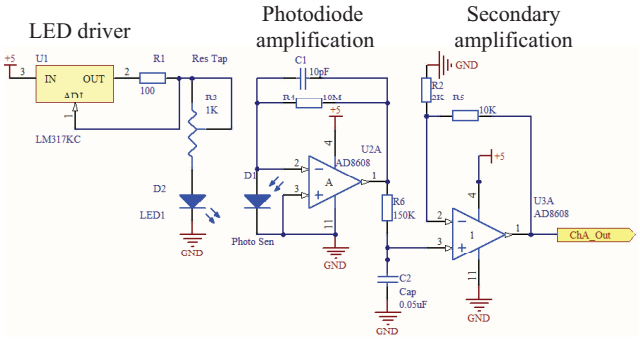

Fig. 7. Circuit diagram of two stage amplification.

The output current from each photodiode is amplified by a quad rail-to-rail operational amplifier (AD8608, Analog Devices Inc., USA), which is further amplified by the same chip as depicted in Fig.7 . To filter out high frequency noise, the output ports of the channels are connected with a simple RC low pass filter (cutoff frequency around $20Hz$). We have built a PCB board to integrate the circuits, and the NI USB6009 data acquisition board is used to perform data readout. A data processing program is written in the NI LabView environment.

IV. Calibration

After the sensor assembly, preliminary force calibration is performed. In the calibration process, the sensor was mounted on a non-vibration table with some designed fixtures. We used some dummy copper weights to apply $100g$ incremental axial forces (up to 9.8 Newton) on the top of sensor. After that, the 8 channel voltage outputs were recorded for 10 seconds. The same procedure was performed to decreasingly unload the weight. The corresponding recorded voltage values were averaged to get the mean voltage output for each channel.

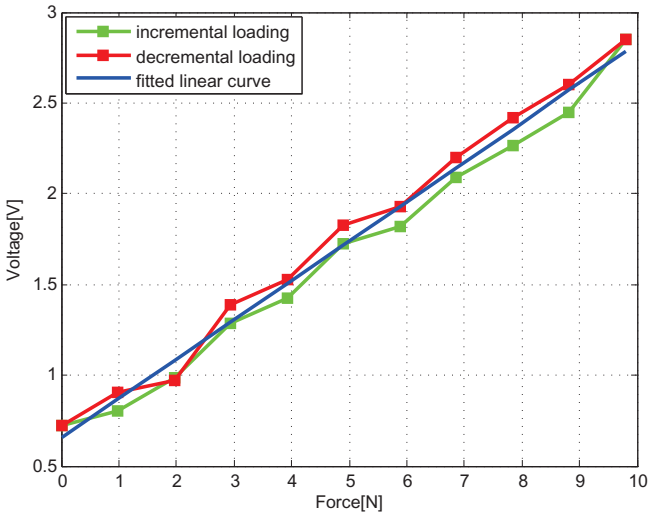

Fig. 8. Response of the sensor to axial loading (along the z direction) with observable hysteresis and the fitted linear curve.

The force/voltage relationship is assumed to be linear and the incremental/decreamental loading data were used to fit a linear curve. The calibration results shown in Fig.8 indicate reasonable linearity (3.33%)and some hysteresis effect can also be observed from the plot.

V. Discussion

Since fiber optic sensors offer high MR compatibility, simple and flexible installation, negligible signal loss and low cost (an FBG for example is very expensive), we choose it as the de facto measurement principle. In this article, we have designed and fabricated a considerably low cost optical force sensor with its sensing principle and structure and performed preliminary experiments to validate its performance.

The linearity, hysteresis and accuracy performance will be reported with the calibration results.

Though the finite element analysis shows the feasibility of the force sensing, further MRI scanner room test should be investigated to further verify the mutual compatibility. The dimension of the sensor is $36mm$ in height and $25mm$ in diameter and it weights $36g$ equipped with $10m$ optical fiber for out scanner room communication. We expect that this sensor can not only be used for needle-based procedures but also generically in other kinds of image guided surgeries, the study of biomechanics, human brain function analysis and rehabilitation study, etc.

On the other hand, some refinements of the sensor design and calibration are possible. A mathematical model of the flexure would facilitate further mechanism optimization. The diameter of the flexure, the number of the fibers, and radius of the fiber to the axis and the distance tolerance of the spherical mirror can be the design variables. With these basic results, in the further development, we would take advantage of higher illuminated LED emitter and sensitive glass optical fibers with polished tips. Another way to attenuate the noise is to use frequency modulated voltage to control the LED intensity while filter out other frequency signal at the output port with some active analog filters. For complicated and time consuming sensor calibration problem, we expect that shape from motion method [14] could provide a better solution and its application is under development.

VI. Acknowledgements

This work is supported in part by the Congressionally Directed Medical Research Programs Prostate Cancer Research Program (CDMRP PCRP) New Investigator Award W81XWH-09-1-0191.

References

[1] G. S. Fischer, I. I. Iordachita, C. Csoma, J. Tokuda, S. P. DiMaio, C. M. Tempany, N. Hata, and G. Fichtinger, "Mri-compatible pneumatic robot for transperineal prostate needle placement," *IEEE/ASME Transactions on Mechatronics*, vol. 13, June 2008.

[2] Y. Wang, G. Cole, H. Su, J. Pilitsis, and G. Fischer, "Mri compatibility evaluation of a piezoelectric actuator system for a neural interventional robot," in *Annual Conference of IEEE Engineering in Medicine and Biology Society*, (Minneapolis, MN), 2009.

[3] `http://www.theprincessgracehospital.co.uk/brachytherapy-how-its-done.php`, 2009 (accessed July 10, 2009).

[4] J. Z. Liu, Z. Luduan, R. W. Brown, and G. H. Yue, "Reproducibility of fmri at 1.5 t in a strictly controlled motor task," *Magnetic Resonance in Medicine*, vol. 52, no. 4, pp. 751–60, 2004.

[5] N. Takahashi, M. Tada, J. Ueda, Y. Matsumoto, and T. Ogasawara, "An optical 6-axis force sensor for brain function analysis using fmri," vol. Vol.1 of *Proceedings of IEEE Sensors 2003 (IEEE Cat. No.03CH37498)*, (Piscataway, NJ, USA), pp. 253–8, IEEE, 2003.

[6] M. Tada and T. Kanade, "Design of an mr-compatible three-axis force sensor," 2005 IEEE/RSJ International Conference on Intelligent Robots and Systems, (Piscataway, NJ, USA), pp. 3505–10, IEEE, 2005. 8750516 MR-compatible force sensor three-axis force sensor optical micrometry MRI displacement sensing optoelectronic devices fiber optics.

[7] T. Tokuno, M. Tada, and K. Umeda, "High-precision mri-compatible force sensor with parallel plate structure," Proceedings of the 2nd Biennial IEEE/RAS-EMBS International Conference on Biomedical Robotics and Biomechatronics, BioRob 2008, (Scottsdale, AZ, United states), pp. 33–38, Inst. of Elec. and Elec. Eng. Computer Society, 2008.

[8] R. Gassert, L. Dovat, O. Lambercy, Y. Ruffieux, D. Chapuis, G. Ganesh, E. Burdet, and H. Bleuler, "A 2-dof fmri compatible haptic interface to investigate the neural control of arm movements," Proceedings. 2006 Conference on International Robotics and Automation (IEEE Cat. No. 06CH37729D), (Piscataway, NJ, USA), pp. 3825–31, IEEE, 2006.

[9] Y.-L. Park, S. Elayaperumal, S. Ryu, B. Daniel, R. J. Black, B. Moslehi, and M. Cutkosky, "Mri-compatible haptics: Strain sensing for real-time estimation of three dimensional needle deflection in mri environments," in *International Society for Magnetic Resonance in Medicine (ISMRM) ,17th Scientific Meeting and Exhibition*, (Honolulu, Hawaii), 2009.

[10] P. Puangmali, K. Althoefer, and L. D. Seneviratne, "Novel design of a 3-axis optical fiber force sensor for applications in magnetic resonance environments," in *IEEE International Conference on Robotics and Automation*, (Kobe, Japan), pp. 3682–3687, 2009.

[11] R. Gassert, D. Chapuis, H. Bleuler, and E. Burdet, "Sensors for applications in magnetic resonance environments," *IEEE/ASME Transactions on Mechatronics*, vol. 13, no. 3, pp. 335–344, 2008.

[12] N. Abolhassani, R. V. Patel, and F. Ayazi, "Minimization of needle deflection in robot-assisted percutaneous therapy," *International Journal of Medical Robotics and Computer Assisted Surgery*, vol. 3, no. 2, pp. 26–34, 2007.

[13] Y. Yu, T. Podder, Y. Zhang, W. S. Ng, V. Misic, J. Sherman, L. Fu, D. Fuller, E. Messing, D. Rubens, J. Strang, and R. Brasacchio, "Robot-assisted prostate brachytherapy," Medical Image Computing and Computer-Assisted Intervention - MICCAI 2006. 9th International Conference. Proceedings, Part I (Lecture Notes in Computer Science Vol. 4190), (Berlin, Germany), pp. 41–9, Springer-Verlag, 2006.

[14] R. M. Voyles Jr, J. D. Morrow, and P. K. Khosla, "Shape from motion approach to rapid and precise force/torque sensor calibration," vol. 57-1 of *American Society of Mechanical Engineers, Dynamic Systems and Control Division (Publication) DSC*, (San Francisco, CA, USA), pp. 67–73, ASME, 1995.